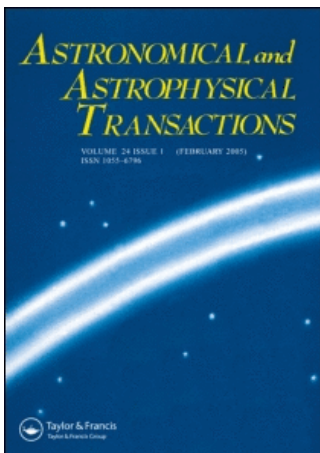


This article was downloaded by:[Bochkarev, N.]
On: 18 December 2007
Access Details: [subscription number 788631019]
Publisher: Taylor & Francis
Informa Ltd Registered in England and Wales Registered Number: 1072954
Registered office: Mortimer House, 37-41 Mortimer Street, London W1T 3JH, UK



Astronomical & Astrophysical Transactions

The Journal of the Eurasian Astronomical Society

Publication details, including instructions for authors and subscription information:
<http://www.informaworld.com/smpp/title~content=t713453505>

The surface of the magnetic CP-Star 21 Per

W. H. Wehlau^a; J. B. Rice^b; V. L. Khokhlova^c

^a Astronomy Department, University of Western Ontario, London, Canada

^b Department of Physics, Brandon University, Brandon, Canada

^c Institute of Astronomy of the USSR Academy of Sci., Moscow, USSR

Online Publication Date: 01 January 1991

To cite this Article: Wehlau, W. H., Rice, J. B. and Khokhlova, V. L. (1991) 'The surface of the magnetic CP-Star 21 Per', *Astronomical & Astrophysical Transactions*, 1:1, 55 - 74

To link to this article: DOI: 10.1080/10556799108244520

URL: <http://dx.doi.org/10.1080/10556799108244520>

PLEASE SCROLL DOWN FOR ARTICLE

Full terms and conditions of use: <http://www.informaworld.com/terms-and-conditions-of-access.pdf>

This article maybe used for research, teaching and private study purposes. Any substantial or systematic reproduction, re-distribution, re-selling, loan or sub-licensing, systematic supply or distribution in any form to anyone is expressly forbidden.

The publisher does not give any warranty express or implied or make any representation that the contents will be complete or accurate or up to date. The accuracy of any instructions, formulae and drug doses should be independently verified with primary sources. The publisher shall not be liable for any loss, actions, claims, proceedings, demand or costs or damages whatsoever or howsoever caused arising directly or indirectly in connection with or arising out of the use of this material.

THE SURFACE OF THE MAGNETIC CP-STAR 21 Per

W. H. WEHLAU§*

Astronomy Department, University of Western Ontario, London, Canada

J. B. RICE*

Department of Physics, Brandon University, Brandon, Canada

V. L. KHOKHLOVA

Institute of Astronomy of the USSR Academy of Sci., Moscow, USSR

Reticon high S/N spectra of CP star 21 Per, obtained with the coude spectrograph of CFHT in Hawaii, were analysed for six phases, homogeneously distributed over the period of rotation. The code of inverse problem solution, by Tikhonov's method, was used to perform doppler imaging of chemical elements Si, Ti, Cr, Mn and Fe on the surface of this star.

Influence of the variation of values of main parameters of analytical representation of local line profiles, as well as variation of values of equatorial velocity, and inclination of rotation axis on final result of imaging procedure, were investigated by extended test computations. It was found that the solution is stable, with respect to variations of all these parameters within the range of their uncertainty.

On the base of this conclusion, we used local equivalent widths to determine local abundances by the model atmosphere method. The maps of distribution of chemical elements are demonstrated.

KEY WORDS Magnetic stars, Chemical abundances.

1. INTRODUCTION

The star 21 Per = HD18269 = HR873 is classified as Ap SiII λ 4200 according to Bertaud (1959). Osawa (1965) gives its hydrogen spectral type as B9p.

Preston (1969) has studied the star spectroscopically and concluded from the profile and equivalent width variations, that chemical elements are distributed over the surface of the star inhomogeneously. According to his study, rare earths as well as titanium and manganese are concentrated in two spots, but silicon, strontium, iron and chromium are distributed more or less homogeneously.

A spectroscopic study of 21 Per by Glagolevskij *et al.* (1976) confirmed Preston's results and also showed that the lines of the elements HgI, WI, OsI,

§ Visiting astronomer. Canada–France–Hawaii Telescope.

* To whom correspondence should be addressed.

AgI and AmII varied periodically, with max. intensity at the maximum light. Maximum light also coincides with the primary intensity maximum of Ti, and lines of rare earths elements.

Stempien (1968) observed the light variations of the star and found a period of 2.883 days, with an amplitude in B of 0.02 mag. Preston (1969) improved the period by studying variations in the intensity of the $\lambda 4012$ line, which is probably the blend of TiII and CrII lines, and gave the ephemeris J.D. (primary maximum) = $2439491.77 \pm 0.03 + (2.88422 \pm 0.00003)E$. Preston also used photometric observations by Stempien and Rakos to draw a new light curve in B and V bands having the amplitude of 0.02 and two maxima at the phases 0.00 (primary) and 0.5 (secondary).

Babcock (1958) measured the magnetic field of 21 Per, and found that it varied from -1270 to $+1350$ Gs; the measurements of the field, when using different lines, appear to give different values. Babcock also noted variability of the line profiles.

New magnetic field measurements were made in 1966 by Preston (1969) and in 1980–1984 by El'kin *et al.* (1987). Preston's data showed scattering from -370 to $+790$ Gs while the estimated error was ± 200 Gs. His data could not be presented by the periodic curve using the period obtained from spectral and photometric variations. Observations by El'kin *et al.* (1984), showed variations from -160 to $+310$ Gs with the error of ± 200 Gs. Nevertheless, they interpreted their results in terms of a sinusoidal curve with a period equal to the photometric one, and with the maximum magnetic field coinciding with light, and R.e. maximum at the phase 0.0. El'kin *et al.* considered two possibilities to explain the decrease in the measured magnetic field since the time of Babcock's observations—an interval of about 30 years. They rejected the first possibility, the precession of the axis of the rotation of the star in a double star system, because the radial velocity did not change from 1966 to 1972. Our observations in 1981 and 1982, also indicate that the radial velocity of 21 Per is constant.

The second possibility considered by El'kin *et al.*, the secular change of magnetic field topology, poses a very interesting question. The general acceptance of the origin of chemical inhomogeneities on the surfaces of CP-stars, the diffusion of elements in the presence of the magnetic field (Michaud *et al.*, 1981), requires a magnetic field to be constant on a time scale of about 100,000 years. The changes of a 10 year timescale would not allow sufficient time for inhomogeneities to form.

Adelman and Pyper (1979) measured energy distribution in the Paschen continuum, and at the Balmer jump. They concluded that the observed distribution could not be described by a single value of T_{eff} . Balmer jump corresponds to $T_{\text{eff}} = 11250$ K, $\log g = 4$, while the Paschen continuum gives $T_{\text{eff}} = 9675$ K, $\log g = 3.75$. The UV colour temperature, as observed by TD-1, was found to be 9400 K (Adelman, 1985). But even using these values, one finds discrepancies between the observed and computed energy distributions. In these determinations of effective temperature, the surface inhomogeneities were not taken into account. That could be, at least in part, the reason of this ambiguity.

Having in mind particular features of 21 Per mentioned above, we think that the mapping of chemical elements on its surface, presents considerable interest.

2. OBSERVATIONS

High-resolution spectra of 21 Per were obtained using the Canada–France–Hawaii telescope with the coude spectrograph and a Reticon detector. The characteristics of this system, as used here, were described earlier (Rice and Wehlau, 1982). The instrumental profile had a full width at half-maximum of 0.09 \AA . Exposure times were generally 30 min; two spectral regions centered on 5040 \AA and 5235 \AA were recorded, each 60 \AA long. The journal of observations is given in Table 1 with the Julian Date of midexposure, the central wavelengths of the spectral region, and the phases as calculated from Preston's ephemeris, as given above.

For the identification and selection of unblended lines to be used in the mapping program, we used the list of lines in the red region of the spectrum of α^2 CVn by Cohen *et al.* (1969), the tables of Moore (1945), Wiese and Martin (1980), and the lists of Kurucz and Peytremann (1975), Kurucz (1981) and Iglezias and Velasco (1964).

The full width at half maximum intensity of lines in the spectrum of 21 Per is about 0.6 \AA at 5000 \AA . In order to measure the radial velocity of the star, to identify the lines accurately, and to estimate the value of $V \sin i$, it was necessary to find the line centers and widths independent of the Doppler shifts, and profile changes that are produced by the inhomogeneities on the surface of the star. To accomplish this, we considered the envelope of the observed profiles, some of which are shown in Figure 1. With this procedure, the line centers were measured with a precision of 0.05 \AA , or better. Thus, using iron and silicon, well identified lines, the radial velocity of 21 Per was determined to be 9.0 km/s , which agrees well with the values of 8.8 and 9.0 km/s found by Preston in 1966 and by Glagolevskij in 1972, respectively.

Within the two spectral regions mentioned above (60 \AA each) we found 14 unblended lines: six of FeII, two of CrII, three of MnII, and one each of TiII, SiII, and one that we were unable to identify ($\lambda = 5286.72$).

Table 1

<i>J.D. 2444000+</i>	$\lambda \text{ \AA}$	<i>Phase</i>
618.8418	5045	0.63
618.8672	5290	0.64
619.7843	5045	0.95
619.8107	5290	0.96
620.7405	5045	0.29
620.7596	5290	0.32
620.8731	5045	0.33
620.8981	5290	0.34
979.8977	5290	0.87
979.9335	5045	0.88
980.7233	5290	0.15
980.7879	5045	0.17
981.7410	5290	0.51
981.7764	5045	0.52

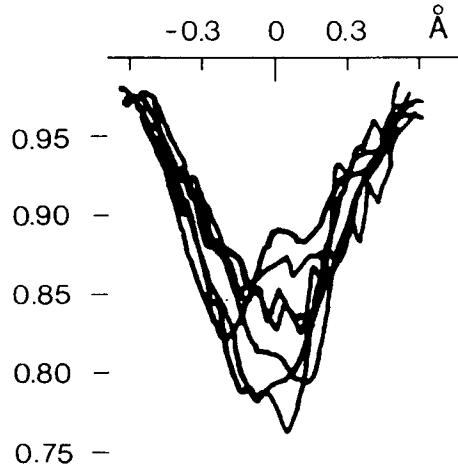


Figure 1 Profiles of the MnII $\lambda 5294.2$ line for seven phases of rotation to draw the envelope (see text).

These lines are listed in Table 2 along with their spectroscopical data (see the comments below in Section 5).

3. DOPPLER MAPPING

Maps of the surface of 21 Per were computed by solving the inverse problem in a manner similar to that previously used. Two versions of the code were used: one was the code OBRA (Goncharskij *et al.*, 1982) used in the Astronomical council of the USSR Academy of Sciences with the computer EC 1045, and the other was written by Rice for use with the VAX computers at Brandon University and the University of Western Ontario (Rice *et al.*, 1989). Both codes give essentially the same results, but the VAX system was much faster, and has a wider range of graphic capabilities, which allowed us to compute more detailed maps and to display them as presented in this paper. In the solution of the inverse problem, we have used an analytical expression for the local line profiles on the star (Goncharskij *et al.*, 1982):

$$r(\lambda) = R_c * \text{TAU}_0 * k(\lambda) / (1 + \text{TAU}_0 * k(\lambda)) \quad (1)$$

where $k(\lambda)$ is the Voigt profile with the parameters GD and GL—Doppler and Lorenz halfwidths. The central depth R_c is approximated by:

$$R_c = C1(1 - \exp(-C2 * \text{TAU}_0)) \quad (2)$$

where TAU_0 corresponds to the optical depth at the center of a line. C1—central depth, R_c , of a very strong line ($\text{TAU}_0 \rightarrow \infty$) and C2 is chosen to give the best fit of R_c values obtained with formula (2) to those computed by integrating the equation of transfer through a model atmosphere. One can find more detailed explanation in the paper by Goncharskij *et al.* (1982).

Table 2

Element	λ	Mult. No	Transition	E_i eV	f_{ik}	Ref	$\sum A_{ik} * 10^{-8}$	$\gamma_C/Ne * 10^{-5}$	Ref.
1	2	3	4	5	6	7	8	9	10
SiII	5041.063	(5)	$4^2P_{1/2}^0 - 4^2D_{3/2}$	10.02	0.74	W	1.95	1.48	JU1
TiII	5037.81	(71)	$b^2D_{5/2} - z^7P_{3/2}^0$	1.57	$0.46 \cdot 10^{-4}$	KP	1.4	0.2	G
CrII	5308.44	(43)	$b^4F_{9/2} - z^4F_{5/2}^0$	4.05	$0.13 \cdot 10^{-2}$	KP	1.32	0.3	G
	5279.92	(43)	$b^4F_{9/2} - z^4F_{7/2}^0$	4.06	$0.87 \cdot 10^{-3}$	KP	2.13	0.3	G
MnII	80.08		$b^7F_{5/2} - z^4F_{7/2}^0$	4.06	$0.90 \cdot 10^{-3}$	KP	2.13	0.3	G
	5294.20	(11)	$e^7D_1 - 4f^7F_5^0$	9.82	0.34	KP	3.1	1.0	JU2
	5295.252	(11)	$e^7D_2 - 4f^7F_2^0$	9.82	0.514	KP	3.56	1.0	JU2
	95.280		$e^7D_2 - 4f^7F_3^0$		0.514	KP	2.34	1.0	JU2
FeII	5296.871	(11)	$e^7D_3 - 4f^7F_5^0$	9.82	0.422	KP	4.1	1.0	JU2
	96.900		$-4f^7F_3^0$		0.422	KP	2.9	1.0	JU2
	96.955		$-4f^7F_4^0$		0.668	KP	5.2	1.0	JU2
	5030.630	—	$4D(5D)6F_{5/2}$	10.29	0.348	KP	10.0	1.0	JU2
	5035.708	—	$-4F(5D)_{4[5]}$	10.29	0.095	KP	10.0	1.0	JU2
			$4D(5D)6D_{5/2}$						
	5061.718	—	$-4F(5D)_{4[5]}$	10.29	0.280	KP	10.0	1.0	JU2
			$4D(5D)6F$						
	5018.43	—	$-4F(5D)_{4[5]}/2$	2.88	0.10	NBS	0.88	0.2	G
			$a^5S_{5/2} - z^6P_{5/2}$						
	5275.95	—	$a^4G_{9/2} - z^4F_{7/2}^0$	3.19	$0.64 \cdot 10^{-4}$	NBS	2.8	0.027	K
	5272.22	—	$7D(5D)2D_{3/2}$	10.41	0.033	K	9.08	1.0	JU2
	5272.397	(185)	$-4P(3F)2D_{5/2}$	5.93	$1.55 \cdot 10^{-2}$	K	4.35	0.0124	K
		$d^2D_{5/2} - 4^2F_{5/2}^0$							

References: W—Wiese, W. L., Smith, M. W., Milis, B. M., 1969; K—Kurucz, 1981; KP—Kurucz and Peytremann, 1975; NBS—Wiese and Martin, 1980; JU1—Jukov, E. A., 1971; JU2—Jukov, E. A. (private communication); G—guess.

In starting the solution we need values for the parameters C1, C2, GD, GL and also for V_{eq} (the equatorial velocity) and i (inclination of the axis of rotation to the line of sight). If incorrect values for these parameters are used in solving the inverse problem, a poor solution can be expected. This will manifest itself by a poor match of the computed line profiles with the observed ones. Some examples of a loss of information that occurs when the values of the parameters used to compute a map deviate from the correct ones, have been given by Rice *et al.* (1989). Although these parameters may be included as quantities to be solved, for the inverse problem solution we have preferred to investigate them separately in order to see the extent to which the final results for 21 Per are influenced by changes in their values.

The appearance of maps of 21 Per and the value of σ , the root mean square deviation of the observed and computed line profiles, serve as a measure of the effects of changes in the values of the parameters.

To investigate this question we computed numerous solutions for the line λ 5295.3 of MnII using different values of the parameters. The results are shown below.

Figure 2 illustrates how σ depends on parameter C2. For C2 between 0.05 and 0.005, the value of σ is almost constant at its minimum value of 0.007 (with σ measured in units of the continuum). The values of W_{max} , written above the points in Figure 2, change by 15% (from 120 to 140 mÅ). Maps produced using values for C2 over the same range, showed only insignificant differences. For further computations we adopted C2 = 0.01.

The parameter C1 corresponds to the central depth of a very saturated line. A numerical solution of the transfer equation using the Kurucz (1979) atmosphere model with $T_{\text{eff}} = 10,000$ K and $\log g = 4.0$ gave C1 = 0.84 at 5000 Å. However, this value for C1 may differ significantly from the true value for 21 Per if the temperature distribution in the star's atmosphere differs significantly from that predicted by an atmosphere model of a normal composition. Figure 3 shows that

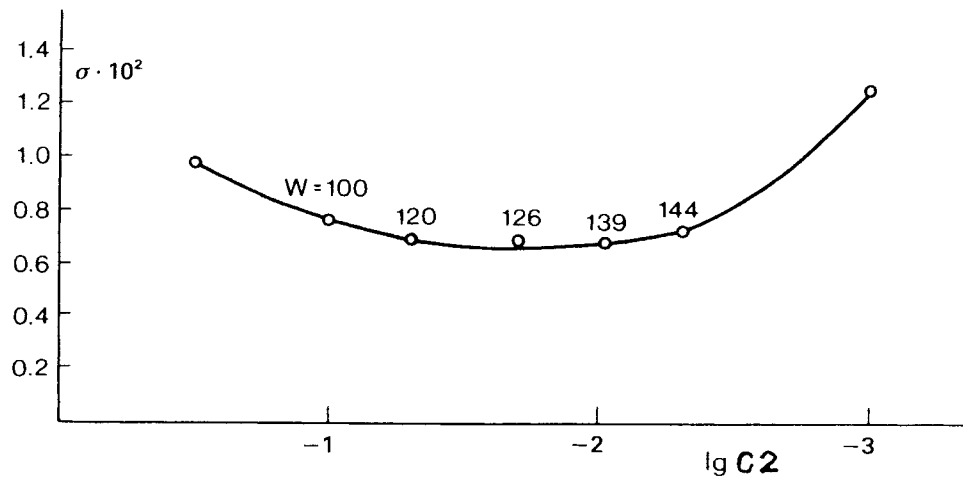


Figure 2 The σ -r.m.sq. deviation of computed profile of the MnII line λ 5295.28 from observed ones for different values of parameter C2.

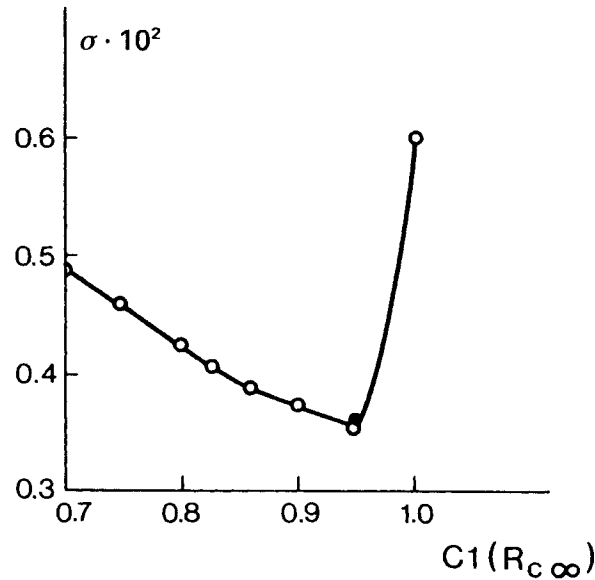


Figure 3 Dependence of σ on the adopted value of parameter $C1$.

σ decreases as $C1$ increases until it reaches a minimum at $C1 = 0.95$, and thereafter σ increases rapidly. Over the range studied, changing $C1$ had little effect on the maps or the local equivalent widths derived. The effect on the maps of changing $C1$ is shown in Figure 4. It appears that an error in the value of this parameter will not have a significant effect on the maps; we adopted $C1 = 0.95$.

Changes in the value of the parameter GD , over the range from 0.02 to 0.04, do not produce substantially different line profiles when expressions (1) and (2) are used (Khokhlova, 1985). Substantial changes in the maps are not expected. This is confirmed by the almost identical appearance of the maps computed with $GD = 0.02$ and 0.03.

The inclination i , enters the computations through the geometrical relations and through the value of $V_{eq} \sin i$, while V_{eq} enters only through this latter term, so it is useful to study how variations in each of these parameters individually affects the maps. The effect of changing the value of V_{eq} (and consequently of $V_{eq} \sin i$), while the other parameters are held constant, as illustrated in Figures 4a, b and c. Figures 4a and 5a show the effect of changing i only. Figures 4a and 4c have considerably different values of $V_{eq} \sin i$, while 4b and 4c have the same value. It is clear from these maps that over the range of uncertainty of V_{eq} and of i the maps do not show any substantial changes if the product $V_{eq} \sin i$ remains constant.

The principal effect is through $V_{eq} \sin i$. Comparing the maps of Figures 4b and 5b, obtained, assuming the same $V_{eq} \sin i$, but different combinations of V_{eq} and $\sin i$, that it is impossible to find any difference with the exception of very small features. However, the increase of the product $V_{eq} \sin i$, drives the spots towards the poles.

The value of $V_{eq} \sin i$ can be obtained readily from the rotational broadening of

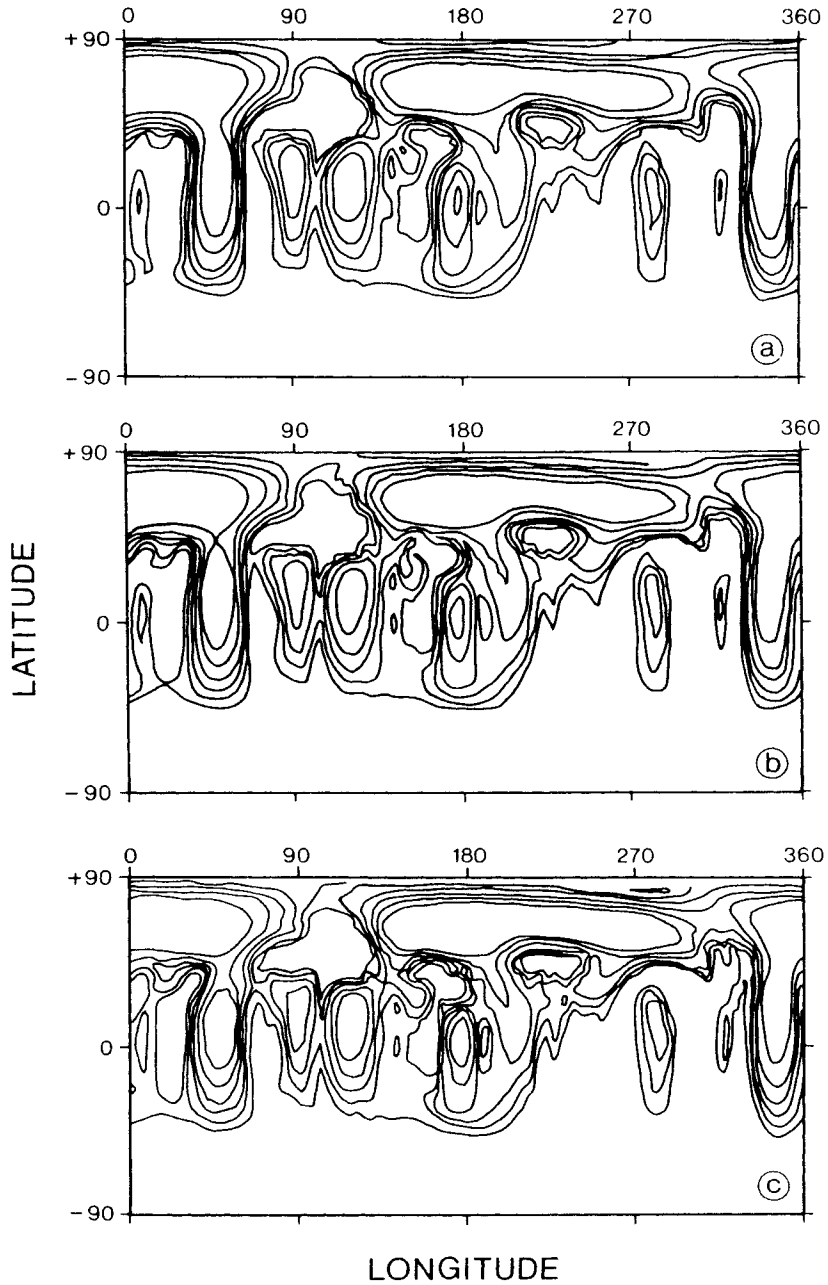


Figure 4 Maps of Mn distribution obtained from $\lambda 5298.28$ line assuming various values of parameter $C1$: a) $C1 = 0.75$; b) $C1 = 0.80$ and c) $C1 = 0.95$. Values of other parameters were: $C2 = 0.01$, $V_{\text{eq}} = 44 \text{ km/s}$, $i = 50^\circ$. Values of σ were obtained: $\sigma = 0.0045$, $\sigma = 0.0043$ and $\sigma = 0.0036$ respectively. Note that the area at latitude $< -i$ is always unseen, and so contain no structure on the maps of Figure 4-9.

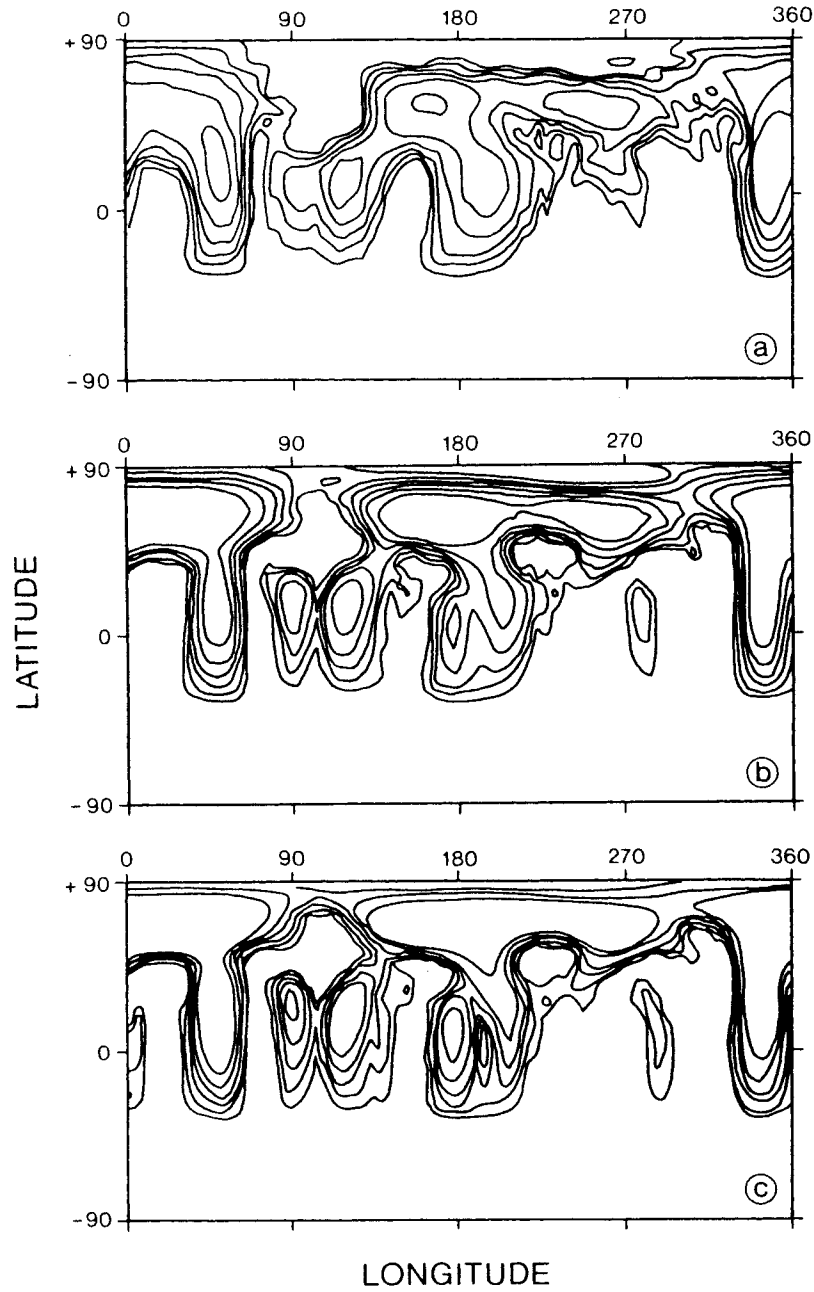


Figure 5 Maps of Mn distribution obtained from $\lambda 5295.28$ line assuming various values of V_{eq} : a) $V_{eq} = 44$ km/s, b) $V_{eq} = 54$ km/s and c) $V_{eq} = 62$ km/s. Values of other parameters were: $C1 = 0.75$, $C2 = 0.01$, $i = 38^\circ$. Obtained values of σ were: $\sigma = 0.0045$, $\sigma = 0.0043$ and $\sigma = 0.0036$ respectively.

an absorption line of an element that is uniformly distributed over the stellar surface. However, for Ap stars there is no assurance that any suitable element is uniformly distributed, not even when equivalent widths of lines are nearly constant with phase. A good estimate of $V_{\text{eq}} \sin i$ can be obtained by the measuring of halfwidths of the envelopes over all phases of a number of lines. Applying this procedure to the relatively strong FeII and SiII lines, we obtained $V_{\text{eq}} \sin i = 25$ km/s. Adopting $2.5R_{\odot}$ as the radius of 21 Per, we obtained $V_{\text{eq}} = 44$ km/s, and $i = 35^{\circ}$.

The insensitivity of the maps to moderate changes in V_{eq} and i , illustrated in Figures 4 and 5, indicates that errors in these values will not lead to large errors in the maps.

These numerical experiments show that the solution of the inverse problem is stable when the parameters mentioned above vary within the range of their uncertainty.

4. MAPS OF ELEMENTS

An objective of the mapping program is to produce maps of the distributions of the elements over the surface of the star. However, to calculate abundances from equivalent widths requires that the correct curve of growth be used at each point on the surface of the star. Since the structure of the atmosphere at each point on a star is not well known, it is best to consider the distributions of the equivalent widths before discussing the distributions of the abundances.

In the case of 21 Per, no substantial variations of temperature or effects of magnetic intensification of lines could be expected. It is convenient, in this

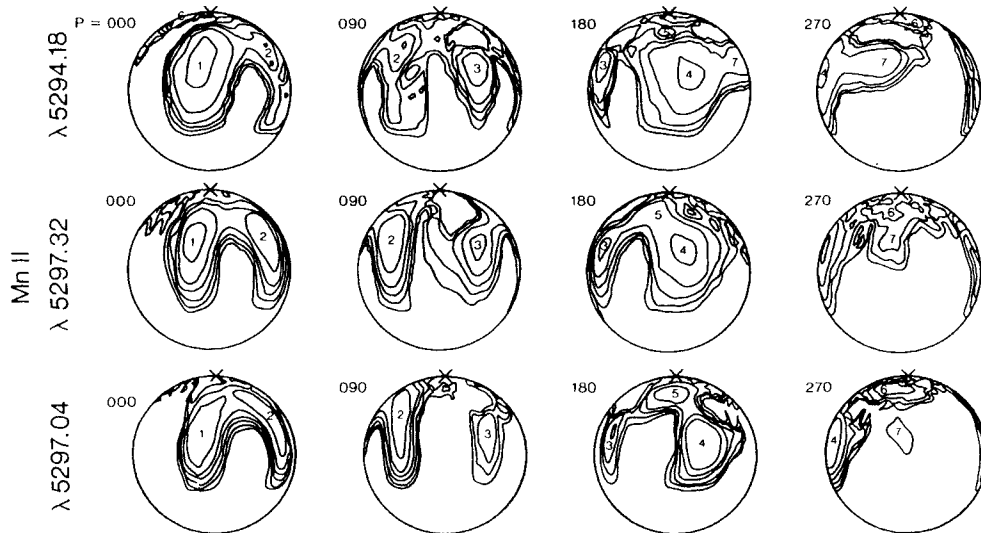


Figure 6 Maps of Mn distribution obtained from MnII lines. The maps in Figures 6–9 are presented for four phases as if the star is seen equator-on. Remember that in computations we adopted $i = 35^{\circ}$, so the lower part of maps ($\varphi < -35^{\circ}$) contain no details because they are invisible and cannot be reconstructed. Numbers indicate seven features as they appear during the rotation period.

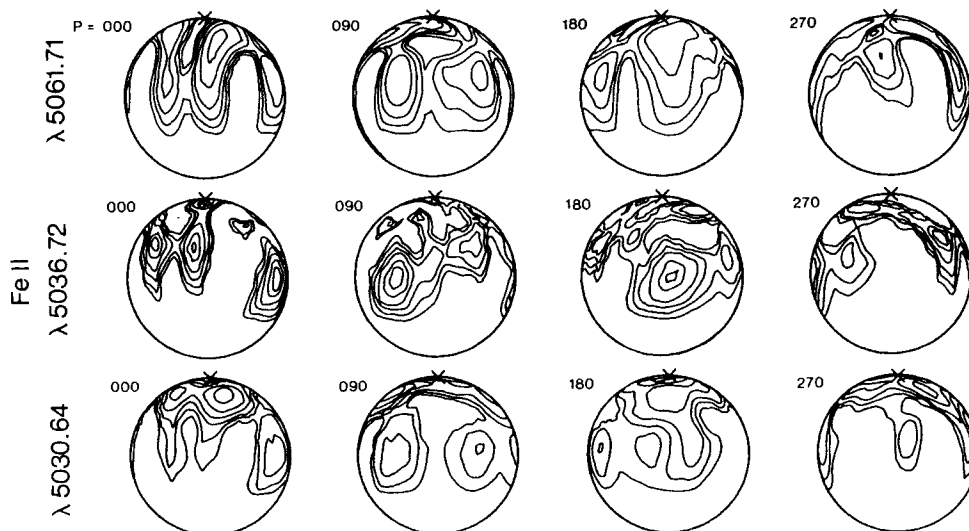


Figure 7 Maps of Fe distribution obtained from 3 FeII lines.

section, to refer to the distribution of the equivalent widths of a particular line, or group of lines, as the distribution of the element which gives rise to that line. Maps of distributions of Si, Ti, Cr, Mn, Fe, and one unidentified element (the line $\lambda 5286.72$), are shown in Figures 6 to 9. Parameters of the maps are summarized in Table 3 and explained in this, and the next, section.

The maps produced from three lines of Mn, and shown in Figure 6, have almost identical distribution. Gradations of the equivalent widths W_{loc} corresponding to isolines are given in Table 3 (upper numbers). The maps of iron distribution are shown in Figure 7. Gradations are also shown in Table 3. The features seen on these maps are quite similar to those of the Mn distribution. A conspicuous difference is seen in the feature that was labelled spot 1 on the Mn maps: on the iron maps it is clearly divided into two parts. The map derived from the $\lambda 5272.3$ line is the most discordant one; this is probably because this line is actually a blend of two FeII lines separated by 0.17 \AA .

The distribution of Cr is shown in Figure 8a. It differs from the distribution of Mn and Fe in several respects. The most important difference can be seen in phase 270° , where the Cr spot is seen, which is located in the area free from Mn, Fe and Si spots. In other phases one can notice some resemblance in distribution of Cr and Mn or Fe, but it is not exactly the same. This is similar to the situation on $\alpha^2 \text{ CVn}$, where the distribution of Cr partly coincides with the distribution of Fe, but some very strong features of Cr are situated at places where the concentration of Fe is the weakest (Khokhlova and Pavlova, 1984).

The map for Si, which was obtained from a single strong line $\lambda 5041$ of SiII, is shown on Figure 8b. This map is smooth with no details, which may be attributed to the saturation of the line over the most part of the stellar surface. The distribution is dominated by two large spots, which generally overlap the main spots of Mn and Fe, but there is no enhancement of silicon around longitude 300 where the strong chromium spot is located.

Table 3

Element	$\lambda, \text{\AA}$	Gradation of isolines in maps (Figure 6-9) in mÅ			Maximal local abundances for $V_t =$			Average W in mÅ for different phases					Average abundances for $V_t =$		Solar abundance			
		150	200	250	300	350	400	3 km/s	2 km/s	0.15	0.32	0.34	0.51	0.64		0.87	0.96	3 km/s
SiII	5041.03	150	200	250	300	350	400	9.46	255	210	223	236	240	229	235	235	9.14	7.52
	5037.81	20	40	60	80	100	120	7.1	27	18	24	30	26	26	30	30	6.15	6.4
	5279.92	50	75	100	125	150	175	7.04	77	77	76	74	76	76	88	79	6.55	5.85
MnII	5308.44	25	50	150	100	125	150	7.54	70	82	115	75	61	71	73	73	6.6	6.8
	5294.20	50	100	75	200	250	300	10.0	126	131	69	135	111	113	127	127	9.0	5.40
	5295.252	25	50	100	100	125	150	8.47	76	71	72	80	64	64	74	74	7.5	
	95.280																	
	2596.87																	
FeII	96.90	60	80	100	120	140	160	8.0	77	70	69	84	72	67	79	79	7.1	
	96.96																	
	5030.64	30	60	90	120	150	170	9.5	74	78	76	79	68	74	76	76	8.4	8.7
	5036.72	20	40	60	80	100	110	9.5	40	29	35	40	35	33	31	31	8.3	8.6
	5061.71	25	50	75	100	125	150	9.5	62	57	57	61	56	58	60	60	8.5	8.8
	5018.43	60	100	140	180	220	260	8.6	176	157	171	169	176	161	149	149	8.0	7.7
	5275.95	30	60	90	120	150	180	7.7	102	93	100	100	103	101	120	120	7.2	7.3
5272.22								63	63	64	63	61	65	76	76	8.4		
?	5286.72	20	50	80	110	140	17	66	59	55	64	59	55	55	55	55	68	

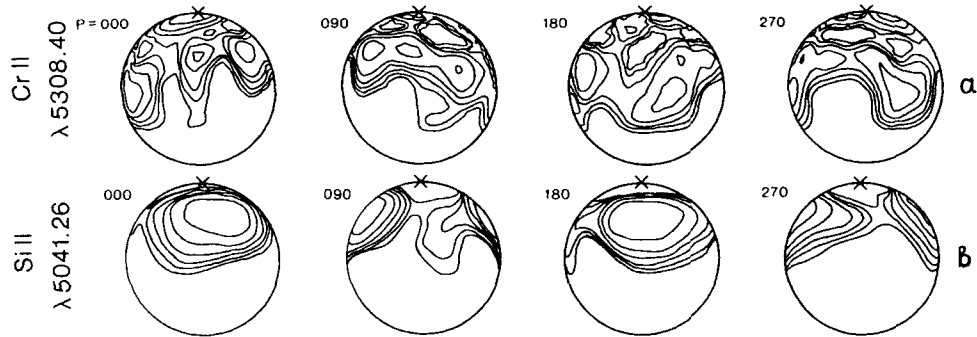


Figure 8 Maps of Cr(a) and Si(b).

Figure 9a is the map of Ti. Figure 9b was produced from the unidentified line $\lambda 5286.72$. Both of these distributions are almost identical to the distribution of Mn.

Our maps may be compared with the previous results for 21 Per by Preston (1969) and by Glagolevskij *et al.* (1976). In both of these papers, the surface distributions of the elements were determined by identifying the individual components within a line, and measuring their radial velocities and strengths. The comparison of our line profiles, Figure 10-12, with those in Preston's Figure 1 shows that similar features and radial velocities would be obtained from our spectra. Two spots of Mn and Ti found by Preston correspond to our spots 1 and 4 (Fig. 6). With the technique used by Preston, detailed maps cannot be produced, so he was unable to identify other features in the Mn and Ti distributions or any of the structure of the distributions of Si, Cr, or Fe. The variations of the line profiles of these elements, shown in Figures 10-12, indicate the difficulty of this procedure.

Glagolevskij *et al.* (1976) obtained results for rare earths, Ti, Mn, Si, Cr and Fe which were the same as Preston's.

5. ESTIMATION OF LOCAL ABUNDANCES

As is shown in Section 3, possible uncertainties in parameters necessary for mapping are not crucial for obtaining maps and local equivalent widths. This

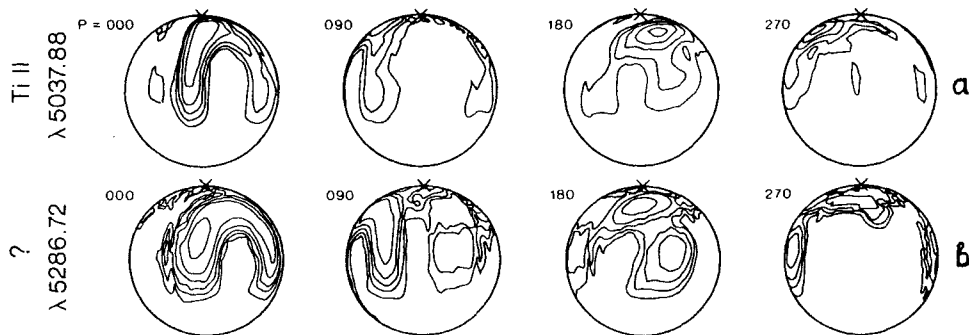


Figure 9 Maps of Ti(a) and one obtained from the line of an unidentified element(b).

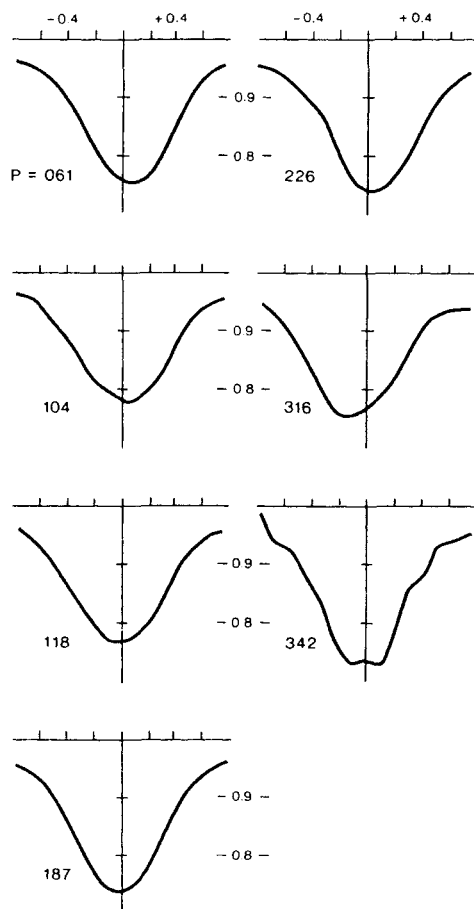
λ 5041.03 Si II

Figure 10 Phase variations of SiII\5041 line profile.

permits us to believe that the values of local W are not far from real ones. So we may attempt to determine local abundances on the surface of CP stars by a traditional fine analysis method. Strictly speaking, this should be done in a selfconsistent way: to use the atmospheric models computed for a particular abundance. But if one uses the lines that are weakly sensitive to temperature, one may use normal atmospheres (Kurucz's for example) as a first approximation. At least, practically, in all determinations of average abundances in CP-stars up to now, this approach is used.

As we are trying to determine the abundance of an element having only one or few lines, it is very important to have reliable values of atomic parameters, such as, oscillator strengths, radiation damping and collisional broadening constants. It is also necessary to be sure that there are no unrevealed blends in the line.

All spectroscopical data for the lines used in this paper are given in Table 2.

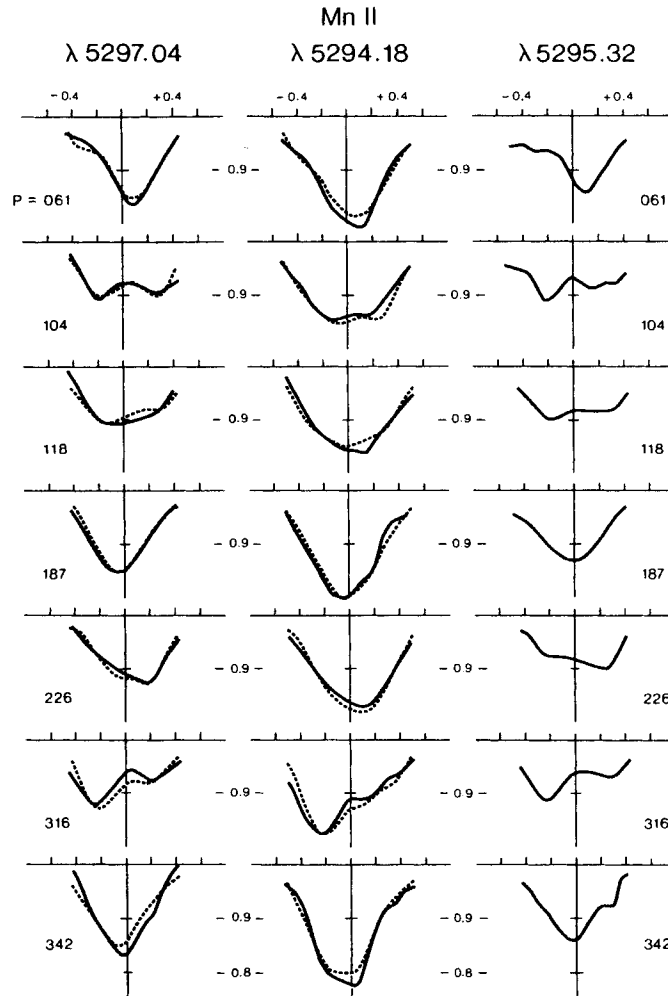


Figure 11 Phase variations of profiles of three MnII lines. Full line-observed profiles, dotted line-computed profiles.

The local equivalent widths, as determined by the solution, are given in Table 3 as gradations of isolines on the maps of Figures 8–10, as well as values of average, that is observed W for all phases.

The theoretical curves of growths were computed for lines given in Table 2 for Kurucz's (1979) atmosphere model with the parameters $T_{\text{eff}} = 10,000$ K, $\log g = 4.0$ and solar chemical composition.

As the maximal values of local W are large enough (from 100 to 300 mÅ), it is necessary to know the broadening constants. Unfortunately, the values of collisional damping for all the lines, but the SiII line, are poorly known.

There are three high excitation lines of iron, classified by Johansson (1978),

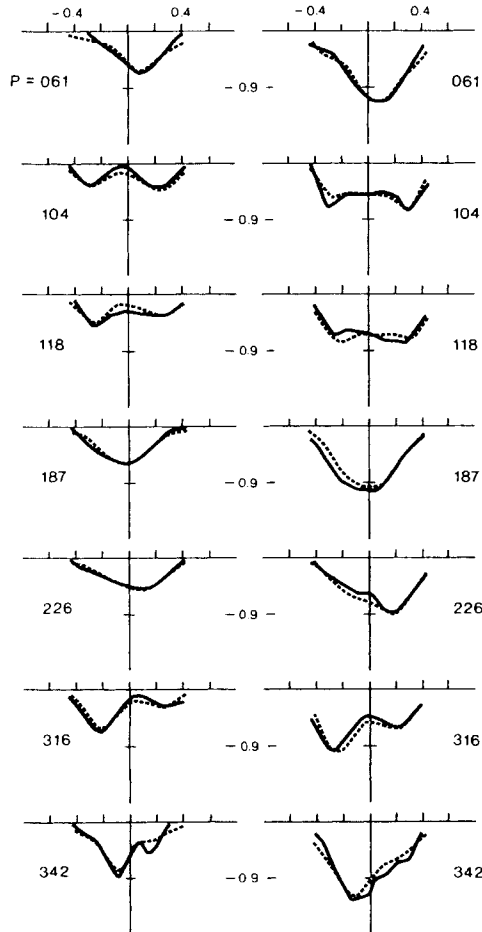
λ 5037.68 Ti II λ 5286.72 ?

Figure 12 Phase variations of profiles of TiII line and the line of unidentified element. Full line—observed profiles, dotted line—computed profiles.

and lines of 11th multiplet of MnII (Iglesias and Velasco, 1964; Kurucz and Peytremann, 1975), which are unblended (Table 2).

Collisional broadening for these lines were computed by E. A. Jukov at the Lebedev Physical Institute, Moscow, and kindly given us, prior to publication. Radiation dumping constants (the sum of A_{ik}) were computed using the Moore (1945, 1950) multiplet tables and Kurucz's and Peytremann (1975) gf -values.

For each element, only very few unblended lines are available. So we could not make any estimates of the microturbulent velocity parameter. The computations were made for V_t equal to 2 km/s and 3 km/s. It is likely that this is an overestimation of V_t . It is known ((Wolff, 1983) that for early A-stars $V_t = 2$ km/s, and for Ap stars, it is expected to be even smaller. As the magnetic field is very weak on 21 Per, magnetic intensification cannot also contribute to the V_t

parameter. Therefore, our abundances should be underestimated rather than overestimated.

The values of the maximal local abundances obtained from the individual lines are given in Table 3 as well as the average abundances obtained from observed W for each phase. One may see that the averages depend weakly on the phase. Average abundances were estimated for the first, and the seventh, phases when the spots 1 and 2 of Mn and Ti are seen near the central meridian, or for the fourth phase when the spot 4 is seen there.

Let us see the results for each element in detail.

Si. The contrast in the obtained distribution of Si is smoothed because the SiII line $\lambda 5041$ is very strong and saturated all over the surface of the star. Average abundance differs from maximal local abundance only for 0.5 dex. The max. local abundance exceeds the solar abundance by more than 100 times.

Ti. Only one line $\lambda 5037.81$ of TiII was used to estimate the abundance of Ti. According to Kurucz and Peytremann's list, the line may be blended by several lines:

5037.77	CeII
5037.81	MnI
5037.813	MnIII
5037.88	CrI

To check if this blending is significant, we computed the equivalent widths of blends using the determined local abundances of Mn and Cr (see below). The contribution of these lines turned out to be negligible. As is known from available line intensity estimations, CeII line must be very weak. However, it is impossible to calculate its contribution, without knowing Ce abundance. In any case, if this line contributes, then the distribution of Ce should be practically the same as that of Ti, since the map obtained from the line $\lambda 5037.81$ coincides with the maps of Mn, and computed profiles fit well to the observed ones (Figure 1). A similar distribution of rare earth elements, Ti and Mn was noted also by Preston (1969).

Maximal local abundance of Ti exceeds the solar value by 2dex. The average abundance is 1dex less than the max. local abundance.

Mn. The abundance was determined using three lines of the same multiplet, one of the lines has double, and another one a triple structure, (see Table 2). The abundance derived from the single line $\lambda 5294.2$ noticeably exceeds the abundances derived from two other lines. Oscillator strengths for all these lines could be found only in Kurucz and Peytremann (1975), and it is difficult to estimate the uncertainty of their data, though it seems that there is no systematic error for MnII in their paper.

For $\lambda 5294.2$ they give smaller gf than for the other two lines, but equivalent widths of this line (average as well as local ones) are systematically higher. (Tables 2 and 3). It is interesting to note, that in spectra of a manganese star, kappa Cnc, this line is weaker (see Aller, 1970), but in spectra of magnetic star α^2 CVn, it is also definitely stronger than others. One may suggest that in the cases 21 Per and α^2 CVn, the line $\lambda 5294.2$ is blended by some unknown line of an element, which is distributed over the surface of the star in the same way as Mn. When excluding the line $\lambda 5294.2$ from consideration we get the mean (from two lines) local abundance of Mn in spot No 1 equal to $8.2 + 0.3$, and average abundance equal to $7.3 + 0.2$.

Cr. Chromium abundance was determined from the single line $\lambda 5308.44$ and the double line $\lambda 5297.92$ and 5298.08 , both components belong to multiplet No43. The maps are not quite similar, but the spot No4 is present in both maps and we estimated the abundance for this spot. The result is shown in Table 3. Note, that the abundance estimated from a double line is almost independent on the assumed value of V_t .

Fe. Three high excitation lines of FeII $\lambda\lambda 5030.63$, 5035.71 and 5061.72 give practically the same local abundance: $9.57 + 0.06$ for $V_t = 3$ km/s and $9.87 + 0.08$ for $V_t = 2$ km/s. The average abundance is determined to be $8.41 + 0.08$ and $8.67 + 0.08$ correspondingly. The line $\lambda 5018.43$ (multiplet No40), for which reliable gf exists from several sources, gives local abundance $8.60/8.66$ and average abundance $7.74/8.04$ for $V_t = 3$ km/s and 2 km/s respectively. This line is rather strong, so the contrast of patches is smoothed. We could not explain such a remarkable discrepancy of iron abundance obtained from lines with different excitation potential, but may suspect that it is due to a wrong temperature run in the atmosphere model used.

6. CONCLUSIONS

The results obtained and described above, permit us to make some conclusions of two different kinds: methodical ones and those that concern the physics of CP stars.

6.1. *Conclusions About the Method*

- 1) Solution of the inverse problem used for doppler mapping is stable with respect to variations of parameters within the range of their uncertainty.
- 2) The local equivalent widths obtained as the result of solving the inverse problem, may be used for estimation of local abundances of chemical elements on the surface of a CP star.
- 3) Due to restricted spectral range available for reticon observations, only very few lines can usually be used for abundance determination. So the lack of atomic data for such lines, and the problem of blending, put, at present time, more difficulties than imperfections of the method of determining the local equivalent widths we used.

6.2. *Conclusions Concerning the CP Star 21 Per*

- 1) The presence of remarkable surface chemical inhomogeneities, when the magnetic field is very weak, is an interesting result. Such inhomogeneities have been found on χ Ser (Gonchariskij *et al.*, 1983) and ϵ UMa (Wehlau *et al.*, 1982), two stars for which most magnetic field measurements have yielded values for the average longitudinal field that are consistent with a zero field or one present only at the level of errors of measurements.
- 2) Maps of an element obtained from different lines of this element do coincide. Particularly good is coincidence of maps of manganese (3 lines) and titanium (1 line). For iron (5 lines) only general features coincide, but worse coincidence is for fine details.

The maximal local abundances in most cases also coincide when determined from different lines, but there are also some discrepancies that are difficult to explain (see Table 3). The maximum local abundance of Mn obtained from $\lambda 5294.2$ MnII is much larger than from the other two lines of the same multiplet. As it was noted in Section 5, this line is probably blended in a spectra of magnetic stars 21 Per and α^2 CVn. Maximal local abundance of iron, determined from three lines originating from the same highly excited level, is practically the same but evidently too high. The reason of difference in abundances obtained from the FeII lines $\lambda 5018.43$ and $\lambda 4275.95$ with well determined gf values is not understood.

There is a large difference between local and averaged abundances of elements. As a rule, maximal local abundances are about 10 times larger than averaged, though variations of the averaged W with the phase of rotation, are very small (see Table 3).

On the surface of the star, regions exist where Si and Ti are overabundant by 2 dex, Cr by 1.3 dex, Fe by 1 dex and Mn by 3 dex.

3) Comparison of geometry of patches obtained in this work with the results obtained earlier by Preston (1969) and Glagolevskij *et al.* showed that the large scale features on the surface of 21 Per are stable. Their position did not change since the years 1963–64 up to 1981–82, that is about 2790 cycles of rotation. One cannot judge about the stability of finer details of surface structure because before 1981 high signal to noise spectra were not available.

4) On the surface of 21 Per, the rough structure of patches is the same for all elements, though some details are different: the strong chromium spot is located at the place free from patches of other elements. The shape of spots No. 1 and No. 2 of Mn is different from the shape of spot No. 1 of iron, situated approximately at the same place. An interesting fact is the simultaneous enhancement of abundance of Mn and Ti, and probably of r.e. elements. In this respect, magnetic CP stars differ from Mn stars, in which R.E. elements are not enhanced along with Mn.

5) It should be desirable in future to continue to observe spectra of 21 Per, exactly in the same spectral regions with the same S/N ratio (about 200–500), each 5–10 years for mapping, and see how stable the distribution of elements is, over the surface of this star.

Acknowledgements

J.B.R. and W.H.W. would like to acknowledge the financial support of the Natural Sciences and Engineering Research Council of Canada. V.L.K. would like to acknowledge the hospitality of the Astronomical Department of UWO, while working there for two months as a guest research scientist.

References

- Adelman, S. J. (1985). *Pasp* **97**, No. 569, p. 970.
Adelman, S. J. and Pyper, D. (1979). *Astron. J.* **84**, No. 11, 1726.
Aller M. F. (1970). *Astron. Astrophys.*, **6**, No. 1, 67.

- Babcock, H. W. (1958). *Astrophys. J. Suppl. Ser.*, **3**, 141.
- Bertaud, C. H. (1959). *Journal des Observateurs*, **42**, No. 4-5, 46.
- Cohgen, J. G., Deutsch, A. J., Greenstein, J. L. (1969). *Astrophys. J.* **156**, 629.
- Glagolevskij, Ju. V., Kozlova, K. I., Lebedev, V. S. and Polosukhina, N. S. (1976). *Astrofizika*, **12**, 631.
- Goncharskij, A. V., Stepanov, V. V., Khokhlova, V. L. and Jagola, A. G. (1982). *Soviet Astronomy*, **59**, No. 6, 1146.
- El'kin, B. G., Glagolevskij, Yu. V., Romanjuk, I. I. (1987). *Izvestija Sao*, **25**, 24.
- Iglesias, L., and Velasco, R. (1964). Publ. del Instituto de Optica Daza de Valdes de Madrid No. 23.
- Johansson, S. (1978). *Physica Scripta* **18**, No. 4, 217.
- Jukov, E. A. (1971). *Sovjet Astronomy* **48**, No. 5, 1094.
- Khokhlova, V. L. (1985). In *Upper Main Sequence Stars with Anomalous Abundances*, ed. Cowley C. R. *et al.*, Reidel Publ. Co, 125.
- Khokhlova, V. L. and Pavlova, V. M. (1984). *Soviet Astronomy Lett.* **10**, No. 3, 377.
- Kurucz, R. and Peytremann, E. (1975). SAO Special Report 362.
- Kurucz, R. (1979). *Astrophys. J. Suppl. Ser.*, **40**, No. 1.
- Kurucz, R. (1981). Sao Special Report 390.
- Michaud, G., Megessier, C. and Charland Y. (1981). *Astron. Astrophys.* **103**, 224.
- Moore, Ch. E. (1945). A Multiplet Tables of Astrophysical Interest, Contr. from the Princeton Univ. Obs. No. 20.
- Osawa, K. (1965). *Ann. Tokyo Astron. Obs. Ser. 2*, **9**, No. 3, 123.
- Preston, G. W. (1969). *Astrophys. J.* **158**, No. 1, 251.
- Rice, J. B., Wehlau, W. H., Khokhlova, V. L. (1989). *Astron. Astrophys.* **208**, 179.
- Rice, J. B. and Wehlau, W. H. (1982). *Astron. Astrophys.* **106**, 7.
- Stempien, K. (1968). *Astrophys. J.* **154**, 945.
- Wehlau, W., Rice, J., Piskunov, N. E. and Khokhlova, V. L. (1982). *Pis'ma v Astronomicheckij Journal*, **8**, No. 1, 30.
- Wiese, W. L. and Martin, G. A. (1980). Wavelengths and Transition Probabilities for Atoms and Atomic Ions, NSRDS-NBS 68.
- Wiese, W. L., Smith, M. W., Miles, B. M. (1969). NSRDS-NBS 22, **11**.
- Wolff, S. C. (1983). The A-Stars: Problems and Perspectives, NASA SP-463, p. 22.